

Dilatonic Black Holes with Gauss-Bonnet Term

Takashi Torii*, Hiroki Yajima† and Kei-ichi Maeda‡

Department of Physics, Waseda University, Shinjuku-ku, Tokyo 169, Japan

(April 12, 2018)

Abstract

We discuss black holes in an effective theory derived from a superstring model, which includes a dilaton field, a gauge field and the Gauss-Bonnet term. Assuming $U(1)$ or $SU(2)$ symmetry for the gauge field, we find four types of spherically symmetric solutions, i.e., a neutral, an electrically charged, a magnetically charged and a “colored” black hole, and discuss their thermodynamical properties and fate via the Hawking evaporation process. For neutral and electrically charged black holes, we find critical point and a singular end point. Below the mass corresponding to the critical point, no solution exists, while the curvature on the horizon diverges and a naked singularity appears at the singular point. A cusp structure in the mass-entropy diagram is found at the critical point and black holes on the branch between the critical and singular points become unstable. For magnetically charged and “colored” black holes, the solution becomes singular just at the end point with a finite mass. Because the black hole temperature is always finite even at the critical point or the singular point, we may conclude that the evaporation process will not be stopped even at the critical point or the singular point, and the black hole will move to a dynamical evaporation phase or a naked singularity will appear.

04.50.+h, 04.70.Bw, 04.70.Dy, 11.15.-q

Typeset using REVTeX

*electronic mail:torii@cfi.waseda.ac.jp

†electronic mail:695L1079@cfi.waseda.ac.jp

‡electronic mail:maeda@cfi.waseda.ac.jp

I. INTRODUCTION

One of the most fascinating dreams for all physicists is the unification of all fundamental forces, i.e., electromagnetic, weak, strong and gravitational interactions. The electromagnetic and weak interactions are successfully unified in the Weinberg-Salam theory. The strong interaction is described by quantum chromodynamics (QCD) and is likely to be unified with the Weinberg-Salam theory into a grand unified theory in the context of gauge theory. The gravitational interaction, however, is not yet included, in spite of a great deal of effort. The most promising candidate for a unified theory of all interactions is a superstring theory, which may unify everything without any divergences.

Although such a unified theory may become important in the strong gravity regime, however, little work has been done on extreme situations such as a black hole or the early universe. Since methods to study the strong gravity regime in a string theory are not well developed, most analysis have been performed by using an effective field theory inspired by a string theory, which contains the leading or next to leading order terms of the inverse string tension α' . One such application is string cosmology. Some puzzles in Einstein cosmology might be solved with a string theory. For example, while the singularity theorem demand that the universe has an initial singularity in the Einstein gravity, a string inspired model can remove it and provide a non-singular cosmology [1,2].

Another application is black hole physics. The first study was made by Gibbons and one of the present authors in the Einstein-Maxwell-Dilaton (EMD) system [3] and the same solution was also discussed in a different coordinate system in ref. [4]. They found a static spherically symmetric black hole solution (GM-GHS solution) with dilaton hair. Since the dilaton hair cannot appear without electromagnetic hair, it is classified as secondary hair. After this work, many solutions were discussed in various models. Thus the following question naturally arises: How are the black hole solutions affected by the next to leading order term in α' , in particular by the higher-curvature term? This was first considered independently of a string theory. Wheeler analyzed the effect of the Gauss-Bonnet (GB) term

without a dilaton field [5]. When the dilaton field is absent, the GB term does not give any contribution in a four dimensional spacetime because it becomes a surface term and gives a topological invariant. Then he studied black holes in spacetime with more than four dimensions. These solutions are called dimensionally continuum black holes [6]. Callan et al. [7] discussed black hole solutions in the theory with a higher-curvature term $R_{\mu\nu\rho\sigma}R^{\mu\nu\rho\sigma}$ and a dilaton field, and Mignemi and Stewart [8] took both the GB term and a dilaton field into account in four dimensional spacetime. In their work, field variables are expanded by the inverse string tension α' and the first order terms of α' are taken into account. Using this perturbation, they constructed analytic solutions. There are also some studies which clarify the effect of an axion field as well as the dilaton field, a U(1) gauge field and the GB term [9–11]. Either dyon solutions or axisymmetric stationary solutions are analyzed because the axion field becomes trivial if the gauge field does not have both electric and magnetic charges and the spacetime is static and spherically symmetric. In all these models containing a higher-curvature term, a perturbative approach was used. Assuming the GB higher curvature term, recently, Kanti et. al. calculated a neutral solution without such a perturbation and found interesting properties [12]. More recently Alexeyev and Pomazanov also discussed the internal structure of these solutions [13].

When we turn to another aspect of a unified theory, we find a non-Abelian gauge field. One of the most important facts about black holes with a non-Abelian gauge field is that we have the so-called colored black hole, which was found in Einstein-Yang-Mills system [14] soon after the discovery of a particle-like Bartnik-McKinnon(BM) solution [15]. These solutions can exist by a balance between the attractive force of gravity and the repulsive force of the Yang-Mills (YM) field. If gravity is absent, such non-trivial structures cannot exist. In this sense, these solutions are of a new type. Although both the BM particle and the colored black hole are found to be unstable against radial linear perturbation [16], they showed us a new aspect of black hole physics and forced us to reconsider the black hole no-hair conjecture.

After these solutions were discussed, a variety of self-gravitating structures and black

hole solutions with a non-Abelian field were found in static spherically symmetric space-time [17–19]. The Skyrmion [20,21] or the Skyrme black hole [22,21,23] in Einstein-Skyrme system, the particle solution with a massive Proca field or the Proca black hole [24] in Einstein-Proca system, the monopole [25–27,19] or the black hole in a monopole [26–28,19] in the Einstein-Yang-Mills-Higgs (real triplet) system and the sphaleron [29,24] or sphaleron black hole [24] in Einstein-Yang-Mills-Higgs(complex doublet) system have been discovered. A particular class of the Skyrme black hole, the Proca black hole and the monopole black hole turns out to be stable against radial perturbations. In particular the monopole black hole can be a counterexample of the black hole no-hair conjecture [19], because it is highly stable and is formed through the Hawking evaporation process from the Reissner-Nordström black hole. We also investigated the dilatonic BM particle and the dilatonic colored black hole solution in the Einstein-Yang-Mills-Dilaton (EYMD) system [23,30], which are direct extensions of the GM-GHS solution.

Although those non-Abelian fields may be expected in some unified theories, such black holes must be very small and then some other contributions such as the GB term and/or the moduli field may also play an important role in their structure, if the fundamental theory is described by a string model. Donets and Gal'tsov showed that a particle-like solution does not exist in the EYMD system with the GB term [31]. Then, they assume a numerical constant β in front of the GB term, where $\beta = 1$ corresponds to the effective sting theory. They showed that there is a critical value $\beta_{cr} = 0.37$, beyond which no particle-like solution exists. However, we expect that a black hole solution can exist in this system, so we also study the case of a SU(2) YM field.

In this paper, then, we study black holes in a theory inspired by a string theory, i.e., in a model with a dilaton field, a gauge field, and the GB curvature term, and discuss their properties. This paper is organized as follows. We outline the a model and field equations in section 2, and present various types of new solutions (neutral, electrically charged, magnetically charged and “colored” black holes) in section 3. In section 4 we study the thermodynamical properties of those black holes. Section 5 includes discussions and

some remarks.

II. A MODEL AND FIELD EQUATIONS

We shall consider the model given by the action

$$S = \int d^4x \sqrt{-g} \left[\frac{1}{2\kappa^2} R - \frac{1}{2\kappa^2} (\nabla\phi)^2 - \frac{1}{6} e^{-2\gamma\phi} H^2 + \frac{\alpha'}{16\kappa^2} e^{-\gamma\phi} (\hat{R}^2 - \text{Tr}\mathbf{F}^2) \right], \quad (1)$$

where $\kappa^2 = 8\pi G$, and discuss a spherically symmetric, static solution. This type of action comes from low-energy limit of the heterotic string theory [32]. The dilaton field is ϕ and $\gamma = \sqrt{2}$ is the coupling constant of the dilaton field to the gauge field. H is a three form expressed as

$$H = dB + \frac{\alpha'}{8\kappa} (\Omega_{3L} - \Omega_{3Y}), \quad (2)$$

where $B_{\mu\nu}$ is the antisymmetric field in the gravitational multiplet. Ω_{3L} and Ω_{3Y} are the Lorentz and gauge Chern-Simon terms respectively;

$$\Omega_{3L} = \text{tr} \left(\omega \wedge R - \frac{1}{3} \omega \wedge \omega \wedge \omega \right), \quad (3)$$

$$\Omega_{3Y} = \text{Tr} \left(\mathbf{A} \wedge \mathbf{F} - \frac{1}{3} \mathbf{A} \wedge \mathbf{A} \wedge \mathbf{A} \right), \quad (4)$$

where the traces are taken over the Lorentz and gauge indices. $\omega_{a\mu\nu} = e_{(a)}^\rho e_\mu^{(b)} \nabla_\rho e_\nu^{(b)}$ is the spin connection with vierbein $e_\mu^{(a)}$. Using the dual of the Bianchi identity, we can rewrite a part of the action

$$-\frac{1}{6} e^{-2\gamma\phi} H_{\mu\nu\rho} H^{\mu\nu\rho} = -\frac{1}{4\kappa^2} e^{2\gamma\phi} \partial_\mu b_{KR} \partial^\mu b_{KR} + \frac{\alpha'}{32\kappa^2} \left[b_{KR} \epsilon^{\rho\sigma\mu\nu} \left(R_{\alpha\beta\rho\sigma} R_{\mu\nu}^{\alpha\beta} + \text{Tr}\mathbf{F}_{\rho\sigma} \mathbf{F}_{\mu\nu} \right) \right]. \quad (5)$$

The pseudoscalar field b_{KR} is the Kalb-Ramond axion. If a spacetime is static and spherically symmetric and the gauge field does not have dyons but only an electric or a magnetic charge, which is the situation we will discuss here, then the second term of equation (5) vanishes. Then the axion field can be regarded as a massless scalar field. Such a scalar field, however,

is trivial because of the black hole no hair theorem [33]. Hence we can drop the axion field here.

\mathbf{F} is the field strength of the gauge field expressed by its potential \mathbf{A} . If it is a $U(1)$ gauge field (the electromagnetic field), then we consider only a electrically or magnetically charged black hole, i.e.,

$$\mathbf{A} = a dt \quad \text{and} \quad \mathbf{F} = \frac{da}{dr} dr \wedge dt. \quad (6)$$

For $SU(2)$ gauge field, we assume the Witten ansatz [34], which is the most generic form of a spherically symmetric $SU(2)$ YM potential. The YM potential becomes

$$\mathbf{A} = a\boldsymbol{\tau}_r dt + b\boldsymbol{\tau}_r dr + [d\boldsymbol{\tau}_\theta - (1+w)\boldsymbol{\tau}_\phi] d\theta + [(1+w)\boldsymbol{\tau}_\theta + d\boldsymbol{\tau}_\phi] \sin\theta d\phi, \quad (7)$$

where a , b , d and w are functions of time and the radial coordinates, t and r . We have adopted the polar coordinate description $(\boldsymbol{\tau}_r, \boldsymbol{\tau}_\theta, \boldsymbol{\tau}_\phi)$, i.e.

$$\boldsymbol{\tau}_r = \frac{1}{2i}[\boldsymbol{\sigma}_1 \sin\theta \cos\phi + \boldsymbol{\sigma}_2 \sin\theta \sin\phi + \boldsymbol{\sigma}_3 \cos\theta], \quad (8)$$

$$\boldsymbol{\tau}_\theta = \frac{1}{2i}[\boldsymbol{\sigma}_1 \cos\theta \cos\phi + \boldsymbol{\sigma}_2 \cos\theta \sin\phi - \boldsymbol{\sigma}_3 \sin\theta], \quad (9)$$

$$\boldsymbol{\tau}_\phi = \frac{1}{2i}[-\boldsymbol{\sigma}_1 \sin\phi + \boldsymbol{\sigma}_2 \cos\phi], \quad (10)$$

whose commutation relations are

$$[\boldsymbol{\tau}_a, \boldsymbol{\tau}_b] = \boldsymbol{\tau}_c \quad a, b, c, = r, \theta, \text{ or } \phi. \quad (11)$$

Here $\boldsymbol{\sigma}_i$ ($i = 1, 2, 3$) denote the Pauli spin matrices. We can eliminate b using a residual gauge freedom. In the static case, the part of the YM equations is integrated as $d = Cw$ where C is an integration constant. We can set $C = 0$ i.e. $d \equiv 0$ without loss of generality. The remaining functions a and w depend only on the radial coordinate r . As a result, we obtain a simplified spherically symmetric YM potential as

$$\mathbf{A} = a(r)\boldsymbol{\tau}_r dt - [1 + w(r)]\boldsymbol{\tau}_\phi d\theta + [1 + w(r)]\boldsymbol{\tau}_\theta \sin\theta d\phi. \quad (12)$$

Substituting this into $\mathbf{F} = d\mathbf{A} + \mathbf{A} \wedge \mathbf{A}$, we find the field strength:

$$\begin{aligned} \mathbf{F} = & \frac{da}{dr} \boldsymbol{\tau}_r dr \wedge dt + \frac{da}{dr} \boldsymbol{\tau}_\phi dr \wedge d\theta + \frac{da}{dr} \boldsymbol{\tau}_\theta dr \wedge \sin\theta d\phi \\ & - (1-w^2) \boldsymbol{\tau}_r d\theta \wedge \sin\theta d\phi + aw \boldsymbol{\tau}_\theta dt \wedge d\theta + aw \boldsymbol{\tau}_\phi dt \wedge \sin\theta d\phi. \end{aligned} \quad (13)$$

Comparing (13) with the field strength of the U(1) gauge field, we find that a and w play the roles of an electric and a magnetic potentials, respectively. This expression can be used for U(1) gauge field if we formally set $\boldsymbol{\tau}_r = 1$ and $\boldsymbol{\tau}_\theta = \boldsymbol{\tau}_\phi = 0$.

The GB term, \hat{R}^2 , is defined by

$$\hat{R}^2 = R_{\mu\nu\rho\sigma} R^{\mu\nu\rho\sigma} - 4R_{\mu\nu} R^{\mu\nu} + R^2. \quad (14)$$

This combination is introduced to cancel anomalies and has the advantage that the higher derivatives of metric functions do not appear in the field equations. Setting $\alpha'/\kappa^2 = 1/\pi g^2$, g is regarded as a gauge coupling constant. A numerical constant β is introduced in Ref. [31] to find a non-trivial particle-like solution, but we fix it to be unity because we are interested in the effective string theory.

Because of our ansatz, the metric is of the Schwarzschild type,

$$ds^2 = - \left(1 - \frac{2Gm}{r}\right) e^{-2\delta} dt^2 + \left(1 - \frac{2Gm}{r}\right)^{-1} dr^2 + r^2(d\theta^2 + \sin^2\theta d\phi^2). \quad (15)$$

The mass function $m = m(r)$ and the lapse function $\delta = \delta(r)$ depend on only the radial coordinate r .

Varying the action (1) and substituting ansätze (12) and (15), we find the field equations;

$$\delta' = h^{-1} \left[-\frac{1}{2} \tilde{r} \phi'^2 - \frac{e^{-\gamma\phi}}{4\tilde{r}} \left\{ e^{2\delta} B^{-2} \tilde{a}^2 w^2 + w'^2 + \frac{2\tilde{m}}{\tilde{r}} (\gamma^2 \phi'^2 - \gamma\phi'') \right\} \right], \quad (16)$$

$$\begin{aligned} \tilde{m}' = h^{-1} & \left[\frac{1}{4} B \tilde{r}^2 \phi'^2 + \frac{e^{-\gamma\phi}}{16} \left\{ e^{2\delta} (\tilde{r}^2 \tilde{a}'^2 + 2B^{-1} \tilde{a}^2 w^2) + 2B w'^2 + \frac{(1-w^2)^2}{\tilde{r}^2} \right. \right. \\ & \left. \left. + 4B \frac{2\tilde{m}}{\tilde{r}} (\gamma^2 \phi'^2 - \gamma\phi'') + 8\gamma\phi' \frac{\tilde{m}}{\tilde{r}^2} \left(B - \frac{\tilde{m}}{\tilde{r}} \right) \right\} \right], \end{aligned} \quad (17)$$

$$\begin{aligned} [e^{-\delta} \tilde{r}^2 B \phi']' - \frac{e^{-\gamma\phi}}{8} \gamma e^{-\delta} \tilde{r}^2 & \left[e^{2\delta} \left\{ \tilde{a}^2 + \frac{2\tilde{a}^2 w^2}{\tilde{r}^2} B^{-1} \right\} - \left\{ \frac{2w'^2}{\tilde{r}^2} B + \frac{(1-w^2)^2}{\tilde{r}^4} \right\} \right. \\ & \left. + \frac{4}{\tilde{r}^2} \left\{ 2f^2 + B(\delta' f + f') \right\} + \frac{4}{\tilde{r}^2} (\delta' f - f') \right] = 0, \end{aligned} \quad (18)$$

$$[e^{\delta} \tilde{r}^2 e^{-\gamma\phi} \tilde{a}']' - 2e^{\delta} e^{-\gamma\phi} B^{-1} \tilde{a} w^2 = 0, \quad (19)$$

$$[e^{-\delta} B e^{-\gamma\phi} w']' + e^{\delta} e^{-\gamma\phi} B^{-1} \tilde{a}'^2 w + e^{-\delta} e^{-\gamma\phi} \frac{w(1-w^2)}{\tilde{r}^2} = 0. \quad (20)$$

Here we have used the dimensionless variables; $\tilde{r} = r/\sqrt{\alpha'}$, $\tilde{m} = Gm/\sqrt{\alpha'}$ and $\tilde{a} = a\sqrt{\alpha'}$.

A prime in the field equations denotes the derivative with respect to \tilde{r} , and

$$B = 1 - \frac{2\tilde{m}}{\tilde{r}}, \quad (21)$$

$$h = 1 + \frac{e^{-\gamma\phi}}{2\tilde{r}}\gamma\phi' \left(B - \frac{\tilde{m}}{\tilde{r}} \right), \quad (22)$$

$$f = h^{-1} \left[\frac{\tilde{m}}{\tilde{r}^2} + \frac{1}{4}B\tilde{r}\phi'^2 - \frac{e^{-\gamma\phi}}{16\tilde{r}} \left\{ e^{2\delta} \left(\tilde{r}^2\tilde{a}'^2 - 2B^{-1}\tilde{a}^2w^2 \right) - 2Bw'^2 + \frac{(1-w^2)^2}{\tilde{r}^2} \right\} \right]. \quad (23)$$

Note that those equations can be applied for a $U(1)$ gauge field by setting

$$w \equiv \pm 1, \quad (24)$$

$$\tilde{a}w \equiv 0, \quad (25)$$

with \tilde{a} being a non-trivial potential. The latter condition (25) corresponds to the vanishing of the self-interaction due to the non-Abelian term.

As for boundary conditions for the metric functions on the event horizon and at spatial infinity, we impose following three ansätze:

- (i) Asymptotic flatness at spatial infinity [35], i.e., as $r \rightarrow \infty$,

$$m(r) \rightarrow M = \text{finite}, \quad (26)$$

$$\delta(r) \rightarrow 0. \quad (27)$$

- (ii) The existence of a regular horizon r_H , i.e.,

$$2Gm_H = r_H, \quad (28)$$

$$\delta_H < \infty. \quad (29)$$

- (iii) The nonexistence of singularities outside the event horizon, i.e., for $r > r_H$,

$$2Gm(r) < r. \quad (30)$$

The subscript H is used for the values at the event horizon $r = r_H$. As for the field functions we have

$$\phi \rightarrow 0, \tag{31}$$

$$a \rightarrow 0, \tag{32}$$

$$w \rightarrow \begin{cases} \pm 1, & \text{(globally magnetically neutral solution).} \\ 0, & \text{(globally magnetically charged solution).} \end{cases} \tag{33}$$

as $r \rightarrow \infty$ and impose their finiteness on the horizon. These conditions guarantee that the total energy of the present system is finite [36]. The boundary conditions of the field functions on the event horizon depend on the gauge group. Hence we will discuss them individually in the next section.

III. NEW DILATONIC BLACK HOLES WITH GAUSS-BONNET TERM

In this section we present the solutions of the field equations (16)~(20). We classified them into four types by their gauge charge, i.e. neutral, electrically charged, magnetically charged and “colored” black holes. All solutions need numerical analysis.

A. Neutral Black Hole

First we consider the case without any gauge field, which is the simplest. The solution is a Schwarzschild type black hole modified by the GB term coupled to a dilaton field. Then the gauge field should be set to

$$\tilde{a} \equiv 0, \tag{34}$$

$$w \equiv \pm 1, \tag{35}$$

which satisfies the field equations (19) and (20). From Eq. (18), we find the following relation for the dilaton field on the event horizon

$$\phi_H'^2 - \frac{\phi_H'}{A\gamma} + 3 = 0, \tag{36}$$

where $A = e^{-\gamma\phi_H}/4\tilde{r}_H^2$. The quadratic equation (36) has two roots as

$$\phi'_{\pm} = \frac{1 \pm \sqrt{1 - 12A^2\gamma^2}}{2A\gamma}. \quad (37)$$

Hence, for each value of ϕ_H at a fixed event horizon \tilde{r}_H , we have two possible boundary values ϕ'_{\pm} .

We integrate the field equations (16)~(18) from the horizon $r = r_H$ with the boundary conditions (28)~(30) and (37). Since the equation of the dilaton field (18) becomes singular on the event horizon, we expand the equations and variables by power series of $\tilde{r} - \tilde{r}_H$ to guarantee the regularity at the horizon, and use their analytic solutions for the first step of integration. We show the behavior of the field functions of neutral black holes with three different radius of event horizon in Fig. 1. We find black hole solutions with a regular horizon only when we choose $\phi'_H = \phi'_+$.

For smaller black holes, the dilaton field varies more rapidly than that of the larger ones. This means that stringy effects become more important for a smaller black hole, as we expected. We see that the mass function decreases first near the horizon and then increases afterward, approaching a finite value. There is a region where the effective energy density, which is defined by $(dm/dr)/4\pi r^2$, becomes negative. From Eq. (17), \tilde{m}' is evaluated on the event horizon as

$$\tilde{m}'_H = -\frac{A\gamma\phi'_H}{2(1 - A\gamma\phi'_H)} = -\frac{1}{6}\phi_H'^2, \quad (38)$$

which is negative definite. Hence the function m always decreases in the vicinity of the event horizon. It is one of the essential points for existence of the neutral black holes that the energy density becomes negative [12]. Regarding the GB term as a source term of the Einstein equations and applying the similar analysis that was used to prove the no-hair theorem for a scalar field, we can show that if the time-time component of the energy-momentum tensor (the effective energy density) is positive everywhere, no non-trivial solution can exist. However in our situation this is not the case. So we find a new solution even if the gauge field is absent.

We show $M - r_H$ relations in Fig. 2. Note that there is an end point for each branch, where ϕ'_+ and ϕ'_- coincide. With this fact, we can prove that ϕ''_H and δ'_H diverge. We have

also shown that $R_{\mu\nu\rho\sigma}R^{\mu\nu\rho\sigma}$ diverges on the event horizon, which means a naked singularity appears at the end point of the branch [12]. We shall call this point the singular point S.

Near the singular point, we also find a critical point C, which gives a lower bound for the black hole mass, i.e., below which mass no solution exists (see Fig. 3(b)). Since this solution is a modification of Schwarzschild black hole, we find no other black hole solutions without a gauge field. No naked singularity appears for the solution at the critical point. We have two black hole solutions in the mass range of $M_C < M < M_S$, where $M_C = 6.02771M_{PL}/g$ and $M_S = 6.02813M_{PL}/g$ are the masses of the critical and singular solutions, respectively. As we will see later, the stability of these black holes changes at the critical point C indicates that the singular end point solution becomes unstable. When we discuss the evolution of the black holes, it will also important be that there exists a regular critical solution whose mass is smaller than that of the singular solution

B. Electrically Charged Black Hole

Electrically charged black hole solutions with the U(1) gauge field can be obtained by setting $w = \pm 1$, $\tilde{a}w = 0$ in Eqs. (16)~(20). Then the electric potential \tilde{a}'' is integrated once to give

$$\tilde{a}' = e^{-\delta} e^{\gamma\phi} \frac{Q_e}{\tilde{r}^2}, \quad (39)$$

where Q_e is a constant of integration and denotes a normalized electric charge. The physical charge is given as gQ_e .

From Eq. (18), we find the following relation for the dilaton field on the event horizon

$$\begin{aligned} & 2A^4\gamma^4 e^{2\gamma\phi_H} Q_e^2 \phi_H'^3 - \left[A^2\gamma e^{2\gamma\phi_H} Q_e^2 (2A^2\gamma^2 + 5A\gamma^2 + 1) - 2A\gamma \right] \phi_H'^2 \\ & + \left[A^4\gamma^2 e^{4\gamma\phi_H} Q_e^4 + Ae^{2\gamma\phi_H} Q_e^2 (2A^2\gamma^2 + 4A\gamma^2 + 1) - 2 \right] \phi_H' \\ & + \left[\frac{A^3\gamma}{2} e^{4\gamma\phi_H} Q_e^4 - A\gamma e^{2\gamma\phi_H} Q_e^2 (6A + 1) + 6A\gamma \right] = 0. \end{aligned} \quad (40)$$

There are three roots of ϕ_H' , $\phi_1' < \phi_2' < \phi_3'$. We can, however, obtain a regular solution only for $\phi_H' = \phi_2'$. This is understood from the fact that in the limit of $Q_e \rightarrow 0$, we recover

the previous condition (36) and $\phi'_3 = \infty$. We plot the field functions of the solutions with $Q_e = 1.0$ in Fig. 3. Their behaviors are almost same as those of the neutral case qualitatively.

We show $M - r_H$ relations of black holes with $Q_e = 0.4$ and 1.0 in Fig. 2. As the neutral black hole case, we also find the critical and the singular points (the end point on the branch), C and S. Fig. 2(c) is a magnification around the critical point C. No singular behavior appears for the critical solution and below the critical point, no solution exists. At the singular point, a naked singularity appears.

The existence of a critical mass is also known in a Reissner-Nordström black hole with a fixed charge. In that case the outer and inner horizons coincide and the black hole becomes extreme at the critical mass. Our solution curve with a constant charge in $M - r_H$ diagram is also vertical at the critical point. However, we will see in the next section that our critical point C has different thermodynamical properties from that of the extreme point in Reissner-Nordström black hole.

C. Magnetically Charged Black Hole

Next we turn to a magnetically charged solution. In the present subsection we extend the gauge field from the U(1) to SU(2) group. This can be done by setting

$$\tilde{a} \equiv 0, \tag{41}$$

$$w \equiv 0. \tag{42}$$

Note that it is not the 'tHooft-Polyakov type, which is obtained through a spontaneous symmetry breaking by a Higgs field as in Refs. [25–28,19], but the Wu-Yang type solution [37]. It is a kind of the dual solution of U(1) electrically charged one. The value of the magnetic charge is quantized as $Q_m = 1.0$.

On the event horizon, Eq. (18) becomes

$$\begin{aligned} & \left[A^3 \gamma^3 (2A + 1) + A \gamma (A - 2) \right] \phi_H'^2 - \left[A^2 \gamma^2 (A^2 + 2A + 2) + (A - 2) \right] \phi_H' \\ & - \frac{A \gamma}{2} (A^2 - 12A + 10) = 0. \end{aligned} \tag{43}$$

We have two roots of ϕ'_\pm but find again a regular solution only for $\phi'_H = \phi'_+$. The behavior of the field functions is similar to that of neutral and electrically charged solutions. We plot the $M - r_H$ relation in Fig. 4. We discuss its properties in the next subsection together with the “colored” case.

D. Dilatonic Colored Black Hole with Gauss-Bonnet Term

Here we set the 'tHooft-Polyakov ansatz $\tilde{a} \equiv 0$, i.e., purely magnetic YM field strength exists. In the SU(2) Einstein-Yang-Mills system, the no-hair theorem for a spherical monopole or dyons was proved [38,39]. It states that there exists no static, spherically symmetric regular non-Abelian black hole solution which has non-zero global Yang-Mills magnetic charge with or without an electric charge. Although it is not clear whether this kind of no-hair theorem holds in the present case, we set $a = 0$ in this paper.

We obtain the following relation on the horizon from Eq. (18),

$$C_1\phi_H'^2 + C_2\phi_H' + C_3 = 0, \quad (44)$$

where

$$C_1 = A^2\gamma(1 - w_H^2)^2(2A^2\gamma^2 + A\gamma^2 + 1) - 2A\gamma, \quad (45)$$

$$C_2 = -A^4\gamma^2(1 - w_H^2)^4 - A(1 - w_H^2)^2(2A^2\gamma^2 + 2A\gamma^2 + 1) + 1, \quad (46)$$

$$C_3 = -\frac{A^3\gamma}{2}(1 - w_H^2)^4 + A\gamma(1 - w_H^2)^2(6A + 1) - 6A\gamma. \quad (47)$$

This has again two roots ϕ'_\pm , and we find a non-trivial solution only with the value ϕ'_+ , as the same as before. The YM equation (20) on the event horizon becomes

$$w_H' = -\frac{w_H(1 - w_H^2)}{2f(r_H)}. \quad (48)$$

Then w_H' is also determined by ϕ_H and w_H . Now we have only one shooting parameter, w_H , which will be fixed by an iterative integration with the boundary condition (33). Here we assume $w_H > 0$ without loss of generality, since the field equations are symmetric for the sign change of w .

With the above conditions, we solve Eqs. (16) ~ (18) and (20) numerically and find discrete families of regular black hole solutions which are characterized by the node number n of the YM potential, just as for the colored black hole [14]. We show some of the solutions with $n = 1$ in Fig. 5. We shall call those solutions “colored” black holes as well. Since the YM field damps faster than $\sim 1/r^2$, those black holes have no global color charge related to the gauge field, just like the colored black hole. Here we use double-quotation marks to distinct our new solutions from the original colored black hole. The dilaton field and metric functions are similar to those of other solutions discussed in the previous subsections. There is a region where the effective energy density becomes negative.

The characteristic feature is that the YM potential w is almost scale invariant. This is recognized as follows. We shall normalize the variables by \tilde{r}_H to see the scale invariance, i.e., $\hat{r} = \tilde{r}/\tilde{r}_H$, $\hat{m} = \tilde{m}/\tilde{r}_H$, $\hat{a} = \tilde{r}_H\tilde{a}$. In the limit of $r\tilde{r}_H \rightarrow \infty$ the field equations become

$$\delta^{\hat{j}} = -\frac{1}{2}\hat{r}\phi^{\hat{j}2} + O\left(\frac{1}{\tilde{r}_H^2}\right), \quad (49)$$

$$\hat{m}^{\hat{j}} = \frac{1}{4}\left(1 - \frac{2\hat{m}}{\hat{r}}\right)\hat{r}^2\phi^{\hat{j}2} + O\left(\frac{1}{\tilde{r}_H^2}\right), \quad (50)$$

$$\left[e^{-\delta}\hat{r}^2\left(1 - \frac{2\hat{m}}{\hat{r}}\right)\phi^{\hat{j}}\right]^{\hat{j}} + O\left(\frac{1}{\tilde{r}_H^2}\right) = 0, \quad (51)$$

$$\left[e^{-\delta}e^{-\gamma\phi}\left(1 - \frac{2\hat{m}}{\hat{r}}\right)w^{\hat{j}}\right]^{\hat{j}} + e^{-\delta}e^{-\gamma\phi}\frac{w(1-w^2)}{\hat{r}^2} + O\left(\frac{1}{\tilde{r}_H^2}\right) = 0. \quad (52)$$

A prime with a hat denotes the derivative with respect to \hat{r} . Eqs. (49) ~ (51) are decoupled from the YM field and are the same as those for the Einstein gravity with a massless scalar field. Because of the no-hair theorem, we find just a Schwarzschild solution with $\phi = 0$. The YM field equation (52) is then the same as that in a fixed Schwarzschild background spacetime, i.e.,

$$\hat{r}(\hat{r} - 2\hat{M})w^{\hat{j}} + 2\hat{M}w^{\hat{j}} + w(1 - w^2) = 0. \quad (53)$$

The non-Abelian YM field can have a nontrivial configuration although it makes no contribution to the black hole structure. Then the solution $w = w^*(\hat{r}) = w^*(\tilde{r}/\tilde{r}_H) = w^*(r/r_H)$ is scale invariant. From our analysis this scale invariance is still found approximately even

for small black holes. The configuration of the YM potentials appears to be described by almost the same function of r/r_H . Although the metric function δ for a small black hole (e.g. $\tilde{r}_H = 1.4007$) varies so rapidly that the above argument may seem to be invalid. This may be understood as follows. δ is decoupled from other field functions even in the original basic equations. As a result the YM potential w is not affected by δ , (see Eq. (53)). Furthermore if $m(r)$ and $e^{-\gamma\phi}$ are almost constant, which is confirmed from our numerical solutions, then the equation for $w(r)$ turns out to be Eq. (53), resulting in a scale invariance of $w(r)$. A similar behavior is found for large black holes in the EYMD system [23].

We show the $M - r_H$ relations of the neutral, the magnetically charged ($Q_m = 1.0$) and the “colored” black holes with node number $n = 1$ in Fig. 6. There exists a lower bound for its mass in each branch. Since the solution does not exist for $r_H \rightarrow 0$, our result is consistent with [31], which says that there is no particle-like solutions in the present system.

Fig. 6(b) is a magnification around the critical point for the magnetically charged and “colored” black hole. Although the neutral and the electrically charged branches have a turning point, which is a critical point, the magnetically charged and “colored” branches do not. The lowest mass corresponds to the end point, where ϕ'_\pm coincide.

Although we have not proved it analytically, we expect that a naked singularity appears at this end point as neutral solutions, because δ' for the black hole near critical mass appears to diverge on the horizon from Fig. 4(d), and in our numerical solutions. Hence the critical point coincides with the singular point S.

IV. THERMODYNAMICAL PROPERTY AND STABILITY

In this section we investigate the thermodynamical properties of the dilatonic black holes with the GB term and then analyze their stability. We also discuss their fates via the Hawking evaporation process.

A. Temperature, Entropy and Stability

The GM-GHS solutions and the non-Abelian black holes have an interesting thermodynamical property. That is, a discontinuity of the heat capacity of the GM-GHS solution appears, depending on the coupling constant of the dilaton field γ . Its critical value is just what we use in this paper [3]. Similar properties were obtained in the EYMD system [23]. Our new black holes may possess similar interesting properties, which is the reason why we investigate the thermodynamical properties here.

Although black hole thermodynamics in non-Einstein theories is not well studied, we can define the temperature and the entropy of the black holes in our model and show that they obey the first law of thermodynamics [40]. The Hawking temperature is given as

$$T = \frac{1}{4\pi r_H} e^{-\delta_H} [1 - 2\tilde{m}'_H], \quad (54)$$

for the metric (15). The inverse temperature $\beta \equiv 1/T$ versus the gravitational mass is shown in Fig. 7. We show the branches of the neutral, the electrically charged ($Q_e = 1.0$), the magnetically charged ($Q_m = 1.0$) and the “colored” black holes with $n = 1$. For comparison we also plot the GM-GHS solution, which have same temperature as Schwarzschild black holes in $\gamma = \sqrt{2}$ case. Comparing the branch of the neutral black holes with that of Schwarzschild black holes, we can guess that the GB term has the tendency to raise the temperature. This can be confirmed by seeing other branches. For example the dilatonic colored black holes in the EYMD system have a lower temperature than that of the Schwarzschild black holes in the mass range of Fig. 7 [23]. However the new solutions with “color charge” are under the branch of the Schwarzschild black holes. These behavior comes from the contribution of \tilde{m}' term of Eq. (54). \tilde{m}' has the minimum value $\tilde{m}' = -1/2$ at the singular point in the neutral case. As for the electrically charged black hole we can see the effect of the GB term in from a different point of view. The thermodynamical properties of GM-GHS solutions changes drastically as the coupling constant γ shifts across $\gamma = \sqrt{2}$. For $\gamma < \sqrt{2}$ the temperature is always lower than Schwarzschild black hole and it vanishes in the extreme limit, while for

$\gamma > \sqrt{2}$ the temperature is always higher than Schwarzschild black hole and it diverges in the extreme limit. For $\gamma = \sqrt{2}$, which is also the applicable value in our case, the temperature coincides with the Schwarzschild case and it is finite even in the extreme limit. However the behavior of the temperature of the electrically charged solutions is similar to the GM-GHS solution with $\gamma > \sqrt{2}$. The critical value of γ in the system including the GB term must be different from $\gamma = \sqrt{2}$ if such a value exists at all.

The effect of the GB term also appears when we discuss the heat capacity. It is always negative for all new black holes found here in spite of the existence of the gauge field. Hence the GB term produces a large effect on the thermodynamical properties.

We also calculate the entropy of our new solutions. Although the entropy is expressed by the quarter of the area of an event horizon in the Einstein theory, this relation cannot be applied in the non-Einstein theory. Here we adopt the entropy proposed by Wald [40], which originates from the Noether charge of the system. This entropy has several desirable properties. For example, it can be defined in a covariant way in all diffeomorphism-invariant theories, which includes the present model, and it obeys the first law of black hole thermodynamics for an arbitrary perturbation of a stationary black hole.

The explicit form of the entropy is derived by

$$S = -2\pi \int_{\Sigma} E_R^{\mu\nu\rho\sigma} \epsilon_{\mu\nu} \epsilon_{\rho\sigma}, \quad (55)$$

where Σ is the event horizon 2-surface, $\epsilon_{\mu\nu}$ denotes the volume element binormal to Σ and the integral is taken with respect to the induced volume element on Σ . $E_R^{\mu\nu\rho\sigma}$ is defined as

$$E_R^{\mu\nu\rho\sigma} = \frac{\partial \mathcal{L}}{\partial R_{\mu\nu\rho\sigma}}, \quad (56)$$

where \mathcal{L} is a Lagrangian density. Substituting the present model (1) into (55) and (56), we obtain a simple form

$$S = \frac{A_H}{4} \left(1 + \frac{\alpha'}{2r_H^2} e^{-\gamma\phi_H} \right), \quad (57)$$

where A_H is the area of the event horizon. This expression is also true for $\gamma = 0$ case, in which we find only a trivial Schwarzschild solution. Although the GB term is totally

divergent for $\gamma = 0$ and does not give any contributions to the field equations, the black hole entropy defined here has the additional constant $\pi\alpha'/2$ via a surface term. Fig. 8(a) is the plots of S/S_{Sch} for new solutions. The entropy of neutral black hole is always larger than that of the Schwarzschild solution with $\gamma = 0$, although the area of neutral black holes is smaller than that of Schwarzschild solutions with a same mass, from Fig. 2. Since ϕ_H is negative for neutral solutions in Fig. 1(a), then the second term of Eq. 57 make the entropy much larger. Similarly, charged black holes have larger entropy than that of Reissner-Nordström solutions. We depict the M - S diagram in Fig. 8(c), which shows the same property as in the Einstein theory that the entropy becomes smaller when the system includes the gauge field.

For the neutral and electrically charged case, we find the critical point C and have two different black hole solutions with the same mass. Since the entropy may be a good indicator for the stability [17–19], we show the fine structure of M - S^* diagram near the critical point in Fig. 8(b) for the neutral black hole. We subtract a linear function which passes through an appropriate point A and the end point S from the entropy $S(M)$ in order to show the structure near the critical point clearly. Hence only the relative values on the vertical axis are significant. We find a cusp structure at the critical point C. The cusp reminds us of the catastrophe theory. Catastrophe theory is a mathematical tool established by Thom to explain a variety of changes of state in nature, in particular a discontinuous change of states which occurs eventually in spite of gradual changes of parameters of a system [41]. It is widely applied in various research fields and in particular we showed that this theory is applicable to the stability analysis of various types of non-Abelian black holes [18,19].

As in the previous non-Abelian black hole case, we adopt the mass and the entropy of a black hole as a control parameter and a potential function, respectively. Then the existence of the cusp structure shows that the stability changes at this point. Then we can conclude that the *upper* branch, AC, is more stable than *lower* branch, CS, since the entropy is the potential function. As a result, the singular point S becomes unstable. Although the stability of the upper branch AC is not confirmed from Fig. 8(c) because the catastrophe

theoretical method gives us only the relative stability, we expect that it is stable since no other solution branch exists. It is also understood from the following argument. We know the stability of the black hole solutions in both EMD and EYMD systems. As in Ref. [31], if we have a numerical constant β in front of GB term, we may have another control parameter β . If we solve a series of black hole solutions from $\beta = 0$ to 1, we find that our present solutions on the AC branch must be stable.

The two curves AC and CS do not intersect with a non-zero angle but become tangent to each other. Since a temperature is expressed by $T = dM/dS$ from the first law of thermodynamics, the temperature is continuous at this critical point. This is consistent with Fig. 7.

Finally, it must be noted, however, that it has not been proved whether the entropy defined by Eq. (55) satisfies the second law of the black hole thermodynamics. In particular in our case there is a region where the effective energy density becomes negative.

B. Fate of Dilatonic Black Holes

We find that the temperature of the black hole is finite for all mass range. Hence we expect that our black holes will not stop evaporating via Hawking radiation. Then we expect the following fates of our black holes: When the neutral or the electrically charged black hole reaches the critical mass C, then the system must shift to another phase which cannot be described as a static spherically symmetric regular black hole. For the magnetically charged and the “colored” black hole, the evaporation proceeds until the spacetime reaches the singular point S and a naked singularity will eventually appear on the hypersurface where the event horizon was located.

However we have to study the evaporation process more carefully. Recall that the temperature of the extreme black hole with $\gamma > \sqrt{2}$ in the EMD system is infinite. Although the naive expectation is that this leads to an infinite emission rate, Holzhey and Wilczek showed that the potential, through which created particles travel away to infinity, grows

infinitely high in the extreme limit, and then it is expected that the emission rate could be suppressed to a finite value [42]. However, it turns out that our numerical analysis shows this expectation is incorrect [43]. In our case, if the potential barrier becomes infinitely large at the critical point C or at the singular point S, the emission rate might be suppressed to zero though the temperature of the black hole remains finite. Then evaporation stops and the black hole cannot reach the critical or the singular point. Therefore we have to calculate the potential barrier for some field in the background of our new solutions.

Here we examine a neutral massless scalar field Φ . It obeys the Klein-Gordon equation;

$$\Phi_{;\mu}{}^{;\mu} = 0. \quad (58)$$

The scalar field is expanded in harmonics. We study one mode of

$$\Phi = \frac{\chi(r)}{r} Y_{lm}(\theta, \phi) e^{-i\omega t}. \quad (59)$$

Eq. (58) becomes separable, and then the radial equation can be written as

$$\left[\frac{d^2}{dr^{*2}} + \omega^2 - V^2(r) \right] \chi(r^*) = 0, \quad (60)$$

where r^* is the tortoise coordinate defined as

$$\frac{d}{dr^*} \equiv \left(1 - \frac{2m}{r} \right) e^{-\delta} \frac{d}{dr} \quad (61)$$

and $V^2(r)$ is the potential;

$$V^2(r) = \frac{e^{-2\delta}}{r^2} \left(1 - \frac{2m}{r} \right) \left[l(l+1) + \frac{2m}{r} - 2m' - r\delta' \left(1 - \frac{2m}{r} \right) \right]. \quad (62)$$

We calculate the potential of the new black holes. We plot the ratio of the black hole temperature to the maximum of the potential for the neutral solution (Fig. 9). We also plot the Schwarzschild black hole case for comparison. All plots for the neutral solutions have larger values than that of Schwarzschild black holes. This result means that the evaporation process of the neutral solution may be faster than in the Schwarzschild case. Of course, the width of the potential is another factor which determines the evaporation rate. However

it does not differ much from that of the Schwarzschild black hole (see Fig. 10). Hence we conclude that the black hole continues to lose its mass, even when the solution approaches the critical mass point or the singular solution one. We then may be faced with a naked singularity, or a transition to a new black hole state (in the neutral or the electrically charged case). Since we have no black hole solutions below the critical mass, the new state might be a time dependent evaporating black hole or just a naked singularity, which was hidden behind the event horizon. It is an open question.

V. CONCLUDING REMARKS

We have studied dilatonic black holes with a GB term and found four new types of solutions, i.e., the neutral, the electrically charged, the magnetically charged and the “colored” black holes. The structures of these black holes and the field configurations are almost the same. This may be because the GB term becomes dominant in the basic equations. As a result, the following previously-unknown properties are found with the GB term:

- (1) The effective energy density becomes negative near the event horizon, which may be responsible for the existence of a new type of black hole.
- (2) The neutral or the electrically charged black holes have the critical point C, below which mass no solution exists, and the singular point S, where a naked singularity appears.
- (3) For the magnetically charged or the “colored” black holes there is no critical point but only the singular point S where the black hole has a finite minimum mass.
- (4) The entropy is calculated. It takes a minimum value at the critical point C for the neutral and electrically charged black holes. We also find a cusp structure in the M - S diagram, which means that the stability changes at the critical point C. Since we do not find a cusp structure for magnetically charged and “colored” black holes, their stabilities do not change.
- (5) The black hole temperature is always finite even at the critical or the singular point. The heat capacity is always negative, like the Schwarzschild black hole, even for the electrically or magnetically charged case. This is because the mass of the extreme black hole without

the GB term, which is given by $GM_{extreme}/\sqrt{\alpha'} = g^2 Q_e$ for a fixed charge, is much smaller than the lower bound for the present black hole mass. Then the charge per unit mass for our black holes is rather small.

(6) From the finiteness of the temperature and the study of the effective potential for a massless scalar field, we may conclude that the evaporation process will not be stopped even at the critical point or the singular point. Hence it seems inevitable that the black hole shifts to another state such as a dynamical evaporation phase or that a naked singularity will appear.

We should mention several further points. There may be a dependence on the metric frame. In this paper we have worked only in the Einstein frame. However some results may change if we go into the string frame since the conformal transformation includes a nontrivial dilaton field. Therefore we studied the system again in the string frame. For example, we plot the $M - r_H$ relation of the neutral black holes in the string frame in Fig. 11. It is known that the gravitational mass and the inertial mass are not equivalent in the string frame. Here we use the former in Fig. 11. We can find similar structures; the existence of a critical point and a singular point. However, the present critical point is not the same as that in the Einstein frame. Since the stability should not change in a choice of the frames, we expect that the entropy will not take a minimum value at this critical point and no cusp structure will appear in the $M_{string}-S_{string}$ diagram. From the consistency for stability analysis, the entropy should be minimized at the critical point in the string frame.

Next is that the solution curve becomes vertical at the critical point in the $M - r_H$ diagram. Hence the rate of change of the size of a black hole becomes infinite there, i.e., if a black hole emits just one particle by the evaporation process (in fact it is possible even at the critical point because the temperature and the effective potential are finite), the size of the black hole will change drastically. This means that the quasi-static approximation is broken and the thermodynamical approach may also break down near the critical point. Thus we have to study this process taking the back reaction into account.

Finally, our results are obtained by using the model (1) which includes only the leading terms of the expansion parameter α' . This expansion may not be valid for Planck scale black holes. The existence and behavior of our black holes near the critical or the singular point will be modified. Hence there is a possibility that the critical and singular point are removed by taking into account the higher or all orders in α' . It might turn out that a particle-like solution found by Donets and Gal'tsov for $\beta < 0.37$ exists in a string theory ($\beta = 1$), which could be important in discussion about the final state of a black hole evaporation or the information loss problem.

– Acknowledgments –

We would like to thank J. Koga and T. Tachizawa for useful discussion and R. Easter for his critical reading of our paper. This work was supported partially by the Grant-in-Aid for Scientific Research Fund of the Ministry of Education, Science and Culture (No. 06302021 and No. 06640412), by the Grant-in-Aid for JSPS Fellows (No. 074767), and by the Waseda University Grant for Special Research Projects.

REFERENCES

- [1] I. Antoniadis, J. Rizos and K. Tamvakis, Nucl. Phys. B **415**, 497 (1994).
- [2] R. Easther and K. Maeda, WU-AP/58/96, hep-th/9605173.
- [3] G. W. Gibbons and K. Maeda, Nucl. Phys. B **298**, 741 (1988).
- [4] D. Garfinkle, G. T. Horowitz and A. Strominger, Phys. Rev. D **43**, 3140 (1991).
- [5] J. T. Wheeler, Nucl. Phys. B **273**, 732 (1986).
- [6] D. L. Wiltshire, Phys. Rev. D **38**, 2445 (1988); B. Whitt, Phys. Rev. D **38**, 3000 (1988);
R. C. Myers and J. Z. Simon, Phys. Rev. D **38**, 2434 (1988); M. Banados, C. Teitelboim
and J. Zanelli, Phys. Rev. D **49**, 975 (1994).
- [7] C. G. Callan, R. C. Myers and M. J. Perry, Nucl. Phys. B **311**, 673 (1988/89).
- [8] S. Mignemi and N. R. Stewart, Phys. Rev. D **47**, 5259 (1993).
- [9] B. A. Campbell, N. Kaloper and K. A. Olive, Phys. Lett. B **285**, 199 (1992).
- [10] B. A. Campbell, N. Kaloper, R. Madden and K. A. Olive, Nucl. Phys. B **399**, 137
(1993).
- [11] S. Mignemi, Phys. Rev. D **51**, 934 (1995).
- [12] P. Kanti, N. E. Mavromatos, J. Rizos, K. Tamvalis and E. Winstanley, hep-th/9511071;
gr-qc/9606008.
- [13] S. O. Alexeyev and M. V. Pomazanov, hep-th/9605106.
- [14] M. S. Volkov and D. V. Galt'sov, Pis'ma Zh. Eksp. Teor. Fiz. **50**, 312 (1989); Sov. J.
Nucl. Phys. **51**, 747 (1990); P. Bizon, Phys. Rev. Lett. **64**, 2844, (1990); H. P. Künzle
and A. K. Masoud-ul-Alam, J. Math. Phys. **31**, 928 (1990).
- [15] R. Bartnik and J. McKinnon, Phys. Rev. Lett. **61**, 141.

- [16] D. V. Galt'sov and M. S. Volkov, Phys. Lett. A **162**, 14 (1992); N. Straumann and Z.-H. Zhou, Phys. Lett. B **234**, 33 (1990); Z.-H. Zhou and N. Straumann, Nucl. Phys. B **234**, 180 (1991); P. Bizon, Phys. Lett. B **259**, 53 (1991); P. Bizon and R. M. Wald, Phys. Lett. B **259**, 173 (1991).
- [17] As a review paper see K. Maeda, Journal of the Korean Phys. Soc. **28**, S468, (1995).
- [18] K. Maeda, T. Tachizawa, T. Torii and T. Maki, Phys. Rev. Lett. **72**, 450, (1994); T. Torii, K. Maeda and T. Tachizawa, Phys. Rev. D **51**, 1510, (1995).
- [19] T. Tachizawa, K. Maeda, and T. Torii, Phys. Rev. D **51**, 4054 (1995).
- [20] T. H. R. Skyrme, Proc. Roy. Soc. London, **260**, 127 (1961); J. Math. Phys. **12**, 1735 (1971).
- [21] S. Droz, M. Heusler and N. Straumann, Phys. Lett. B **268**, 371 (1991); P. Bizon and T. Chmaj, Phys. Lett. B **297**, 55 (1992).
- [22] H. C. Luckock and I. Moss, Phys. Lett. B **176**, 314 (1986); H. C. Luckock, *String Theory and Quantum Gravity* ed. by H. J. de Vega and N. Sanchez, (World Scientific, 1987), p.455.
- [23] T. Torii and K. Maeda, Phys. Rev. D **48**, 1643 (1993).
- [24] B. R. Greene, S. D. Mathur and C. M. O'Neill, Phys. Rev. D **47**, 2242 (1993).
- [25] G. 'tHooft, nucl. Phys. B **79**, 276 (1974); A. M. Polyakov, Pis'ma Zh. Eksp. Teor. Fiz. **20**, 430 (1974).
- [26] K. -Y. Lee, V. P. Nair and E. Weinberg, Phys. Rev. Lett. **68**, 1100 (1992); M. E. Ortiz, Phys. Rev. D **45**, R2586 (1992).
- [27] P. Breitenlohner, P. Fargács and D. Maison, Nucl. Phys. B **385**, 357 (1992).
- [28] P. C. Aichelburg and P. Bizon, Phys. Rev. D **48**, 607 (1993).

- [29] R. Dashen, B. Hasslacher and A. Neveu, Phys. Rev. D **10**, 4138 (1974); N. S. Manton, Phys. Rev. D **28**, 2019 (1983); F. R. Klinkhamer and N. S. Manton, Phys. Rev. D **30**, 2212 (1984).
- [30] G. Lavrelashvili and D. Maison, Phys. Lett. B **295**, 67 (1992); Nucl. Phys. B **410**, 407 (1993); E. E. Donets and D. V. Gal'tsov, Phys. Lett. B **302**, 411 (1993).
- [31] E. E. Donets and D. V. Gal'tsov, Phys. Lett. B **352**, 261 (1995).
- [32] D. Gross and J. H. Sloan, Nucl. Phys. B **291**, 41 (1987).
- [33] J. d. Bekenstein, Phys. Rev. D **5**, 1239;2403 (1972); *ibid* **51**, R6608 (1995).
- [34] E. Witten, Phys. Lett. **38**, 121 (1977).
- [35] In our analysis, we set

$$\begin{aligned}\delta_H &= 0, \\ \delta(r) &\rightarrow \delta_\infty = \text{const.} \quad \text{as } r \rightarrow \infty,\end{aligned}$$

instead of the condition (27) in order to simplify the numerical calculations. This difference in δ is recovered by rescaling the time coordinate as $t \rightarrow te^{\delta_\infty/2}$.

- [36] Since the value of the dilaton field ϕ is not fixed up to a constant because the constant difference can be absorbed in the radial coordinate by rescaling, we can relax the condition (31). For example, we can assume that the dilaton field approaches to some unknown constant value ϕ_∞ as $r \rightarrow \infty$. Introducing $\bar{\phi}$ defined by $\bar{\phi} \equiv \phi - \phi_\infty$, and rescaling the variables as $\bar{r} = e^{-\gamma\phi_\infty/2}\tilde{r}$, $\bar{m} = e^{-\gamma\phi_\infty/2}\tilde{m}$ and $\bar{a} = e^{\gamma\phi_\infty/2}\tilde{a}$, we find our boundary condition. However, in our numerical analysis, because we have fixed a charge of black hole in each branch, we have to search for the value of ϕ_H by use of an iteration method such that ϕ_∞ vanishes. Otherwise a must be rescaled if $\phi_\infty \neq 0$, giving a different value of charge. Hence ϕ_H is not a free parameter but a shooting parameter in the electrically charged black hole case.

- [37] T. T. Wu and C. N. Yang, *Properties of matter under unusual conditions*, (Interscience, New York, 1969), p.349.
- [38] A. A. Ershov and D. V. Gal'tsov, Phys. Lett. A **150**, 159 (1993).
- [39] P. Bizon and Q. T. Popp, Class. Quantum Grav. **9**, 193 (1992).
- [40] R. M. Wald, Phys. Rev. D **48**, R3427 (1993); V. Iyer and R. M. Wald, Phys. Rev. D **50**, 846 (1994).
- [41] R. Thom, *Structural Stability and Morphogenesis*, Benjamin (1975).
- [42] C. F. E. Holzhey and F. Wilczek, Nucl. Phys. B. **380**, 447 (1992).
- [43] J. Koga and K. Maeda, Phys. Rev. D **52**, 7066 (1995).

Figure Captions

- FIG. 1: We plot the behavior of (a) the dilaton field (b) the mass function and (c) the lapse function of the neutral black holes for three different radii of event horizon; $r_H/\sqrt{\alpha'} = 1.5704$ (solid line), $= 1.9784$ (dotted line), $= 3.0556$ (dashed line). We find the region where the effective energy density becomes negative. δ' seems to diverge on the event horizon as the black hole gets smaller.
- FIG. 2: (a) The mass-horizon radius diagram for the neutral black holes ($Q_e = 0$) and the electrically charged black holes ($Q_e = 0.4, 1.0$). There is an end point, where a naked singularity appears, for each curve. We also plot the Schwarzschild black hole and the GM-GHS solution for comparison. (b) and (c) is a magnifications around the singular point S of neutral black holes and electrically charged black holes respectively. We find the critical point C, below which no solution exists.
- FIG. 3: We plot the behavior of (a) the dilaton field (b) the mass function and (c) the lapse function of the electrically charged black holes with $Q_e = 1.0$ for three different radii of event horizon; $r_H/\sqrt{\alpha'} = 1.52$ (solid line), $= 1.70$ (dotted line), $= 2.00$ (dashed line). The qualitative behaviors of these functions are almost same as those of the neutral case.
- FIG. 4: We plot the behavior of (a) the dilaton field (b) the mass function and (c) the lapse function of the magnetically charged black holes with $Q_m = 1.0$ for three different radii of event horizon; $r_H/\sqrt{\alpha'} = 1.3864$ (solid line), $= 1.8929$ (dotted line), $= 3.0101$ (dashed line). The qualitative behavior of these functions is almost same as that of the neutral and electrically charged case.

FIG. 5: We plot the behavior of (a) the dilaton field (b) the mass function (c) the lapse function and (d) the YM potential of the “colored” black holes for three different radii of event horizon; $r_H/\sqrt{\alpha'} = 1.4007$ (solid line), $= 1.8964$ (dotted line), $= 3.0117$ (dashed line). The behavior of the YM potential w hardly depends on the size of the black hole. The Yang-Mills field damps faster than $\sim 1/r^2$ so “colored” black holes have no global YM charge.

FIG. 6: (a) The mass-horizon radius diagram for the neutral, the magnetically charged ($Q_m = 1.0$) and “colored” black holes ($n = 1$). We plot the Schwarzschild black holes and GM-GHS solutions for comparison. There exists a lower mass for each branch. (b) is a magnification around the end points of magnetically charged and “colored” black holes. There is no critical point but only the singular point, where a naked singularity appears.

FIG. 7: The mass-temperature relations for the neutral, the electrically charged ($Q_e = 1.0$), the magnetically charged ($Q_m = 1.0$) and the “colored” black hole ($n = 1$). The temperature remains finite in all mass range for each branch. The effect of the GB term also appears in the heat capacity, which is always negative for each branch in spite of the existence of the gauge field.

FIG. 8: (a) We plot the ratio of the entropy for the neutral, the electrically charged ($Q_e = 1.0$), the magnetically charged ($Q_m = 1.0$) and the “colored” black hole ($n = 1$) to that for the Schwarzschild black hole. Here we define the entropy of the Schwarzschild black hole by Eq. (57), so it contains the contributions of a surface term. We plot the entropy of Reissner-Nordström black holes by dashed line for comparison. The neutral and the charged solutions have larger entropy than Schwarzschild and Reissner-Nordström black holes respectively. (b) is the entropy for these four types of solutions. The entropy becomes small when the system includes the gauge field. This behavior is same in Einstein theory. (c) is the magnification around the critical point of the neutral black holes. We change the vertical axis $S \rightarrow S^*$ in order to show the structure clearly by subtracting the linear function, which passes through the points A and S, from the original entropy S . Hence the absolute value have no meaning. We can find a cusp structure, which means that the stability change occurs at the critical point C.

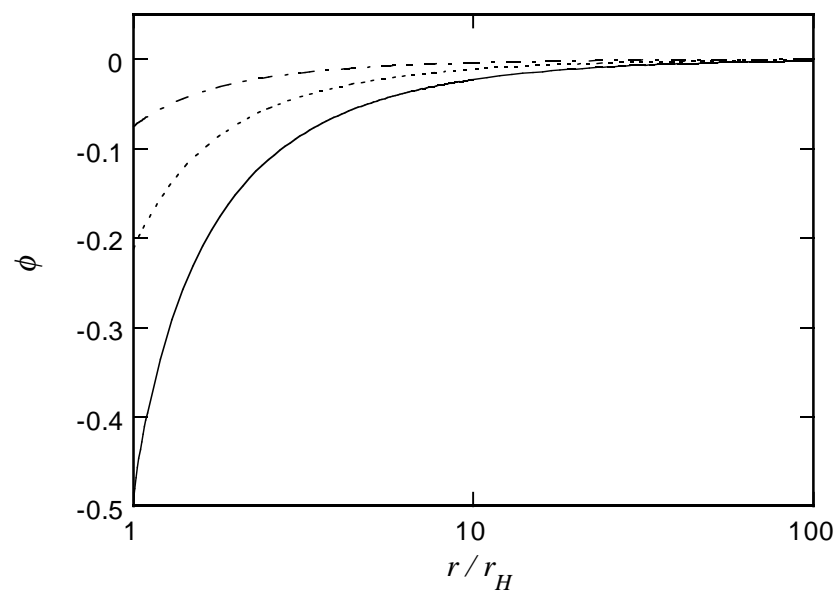
FIG. 9: The ratio of the temperature to the maximum of the potential, through which particles travel, of the neutral black holes. The ratio of new solutions is always larger than that of the Schwarzschild black hole. Hence the evaporation proceeds until the black hole reaches to the critical point.

FIG. 10: We plot the configurations of the potential of neutral massless scalar field around the neutral black holes with three different radii of the event horizon; $r_H/\sqrt{\alpha'} = 1.5704, = 1.9784$ and $= 3.0556$. We also plot those of the Schwarzschild solution case with the same size of black hole as each neutral solution. The configurations are similar to those of Schwarzschild solutions for all horizon sizes.

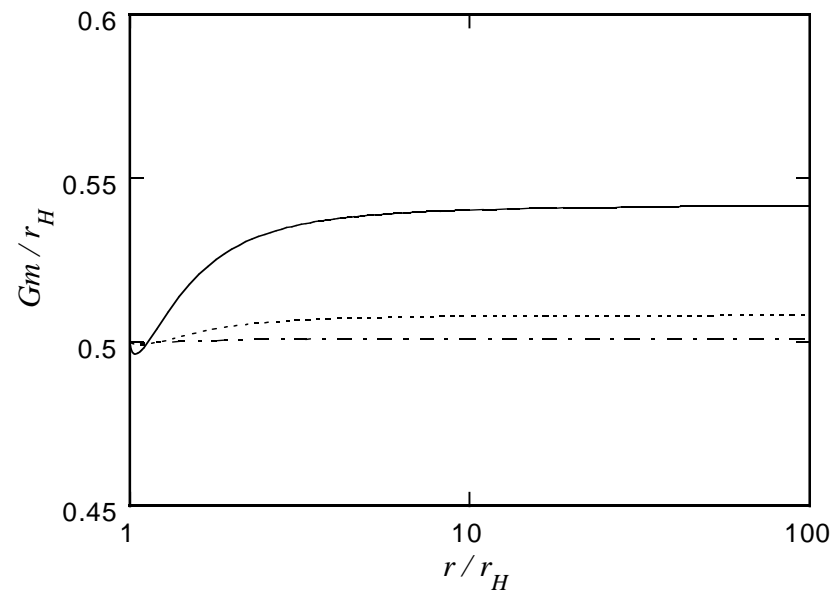
FIG. 11: The mass-horizon radius diagram for the neutral black holes in the string frame. There are also both critical and singular points. This critical point, however, does not coincide with that in Einstein frame.

fig.1

(a)



(b)



(c)

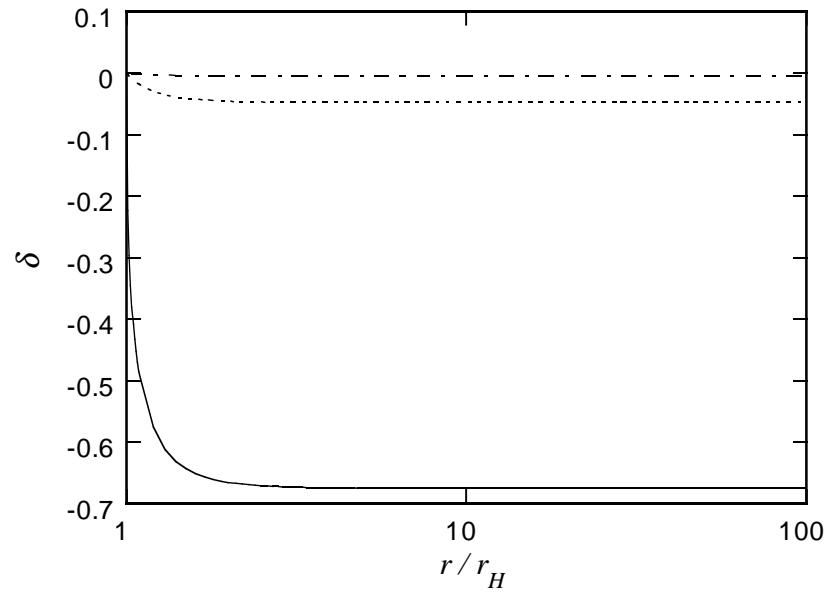


Fig.2

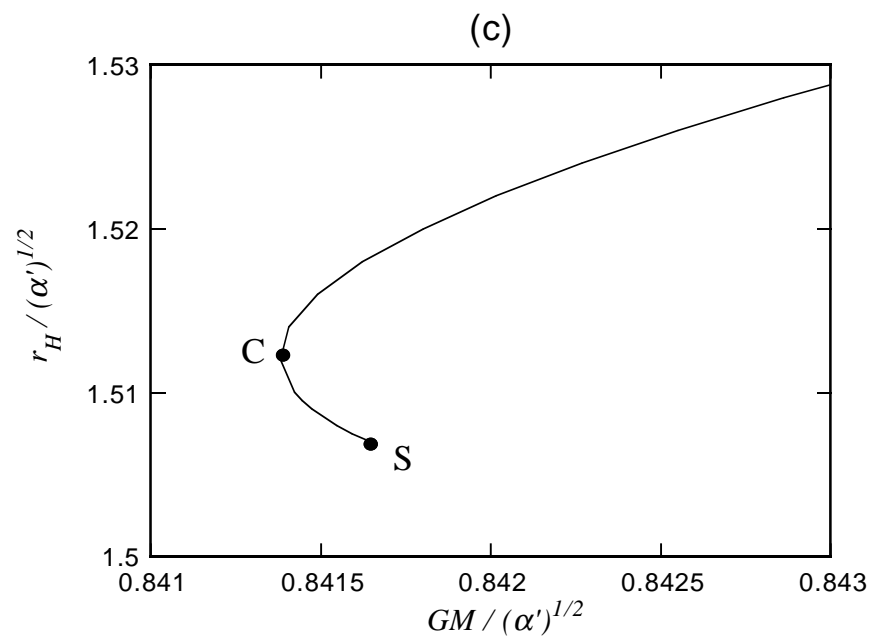
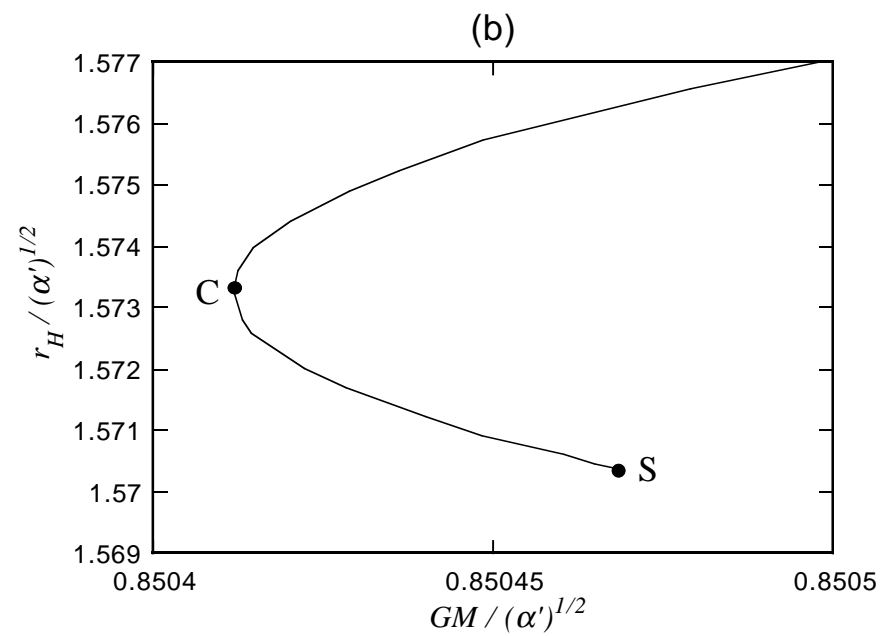
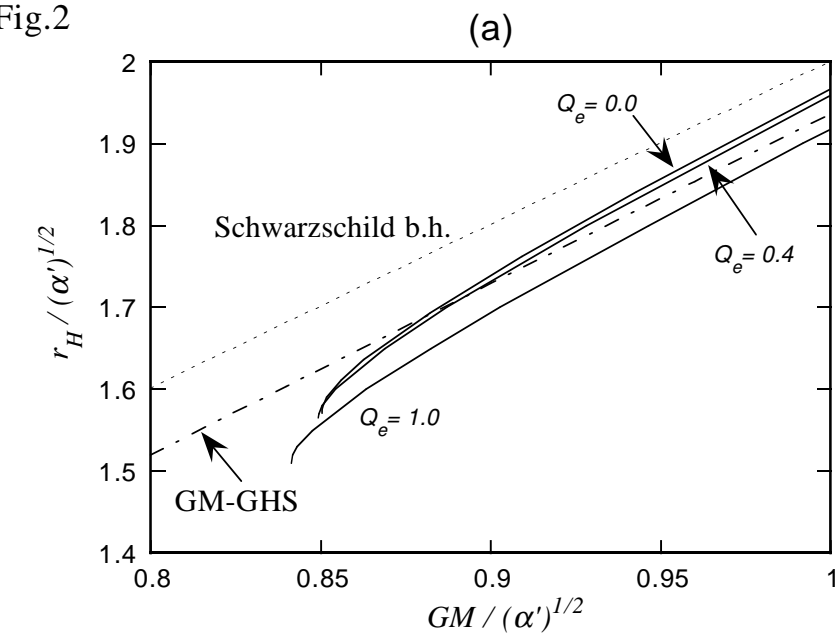


Fig.3

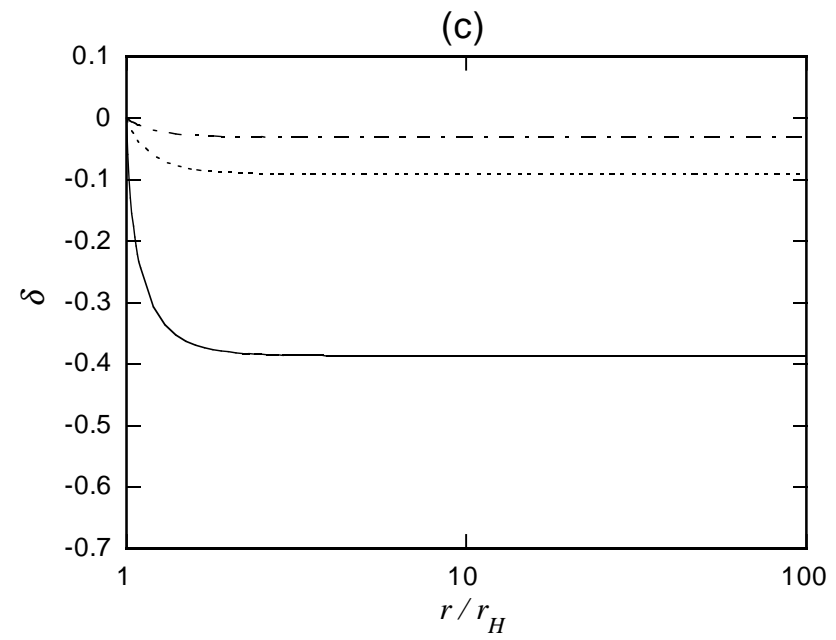
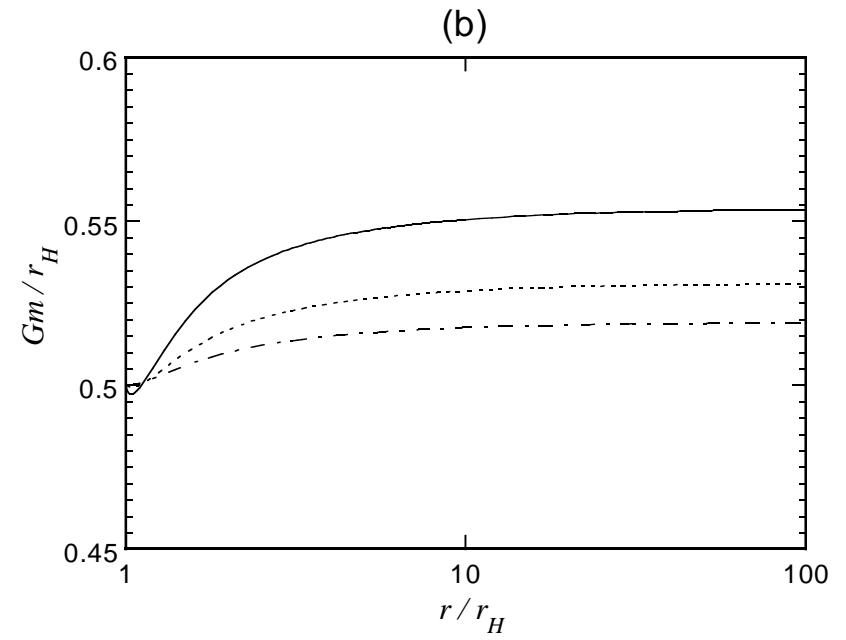
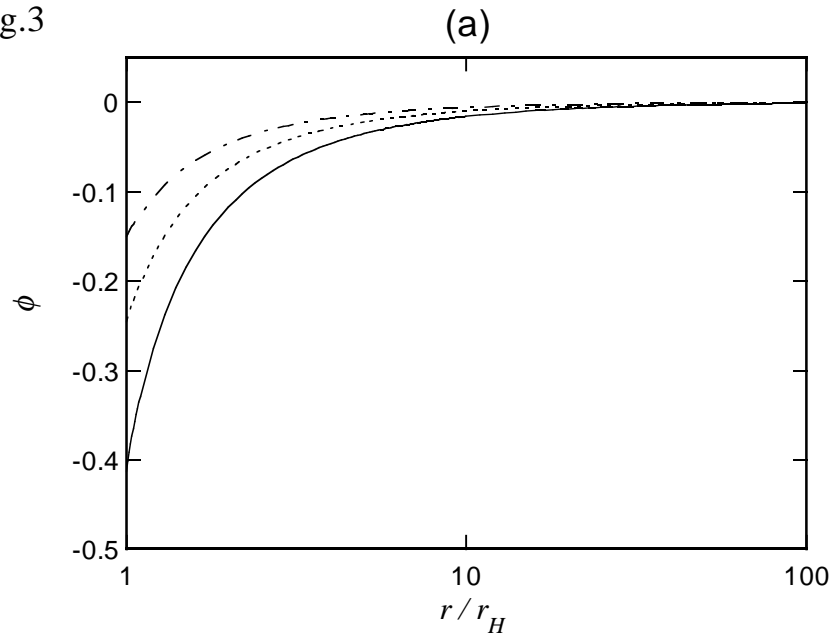


Fig.4

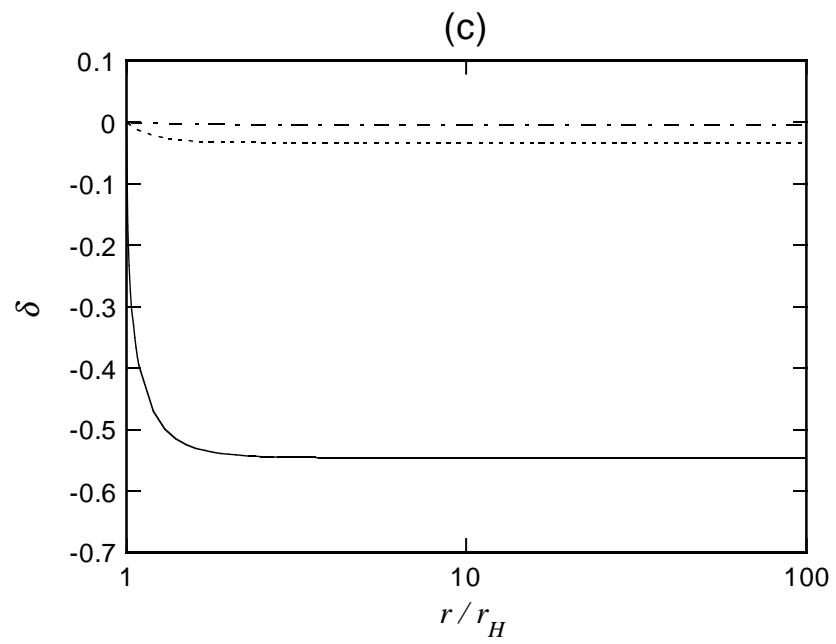
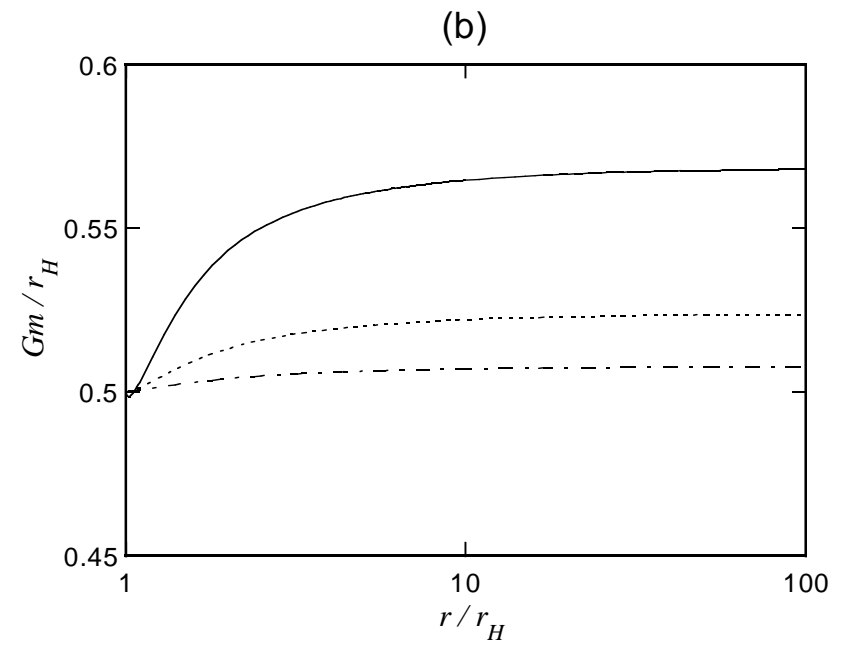
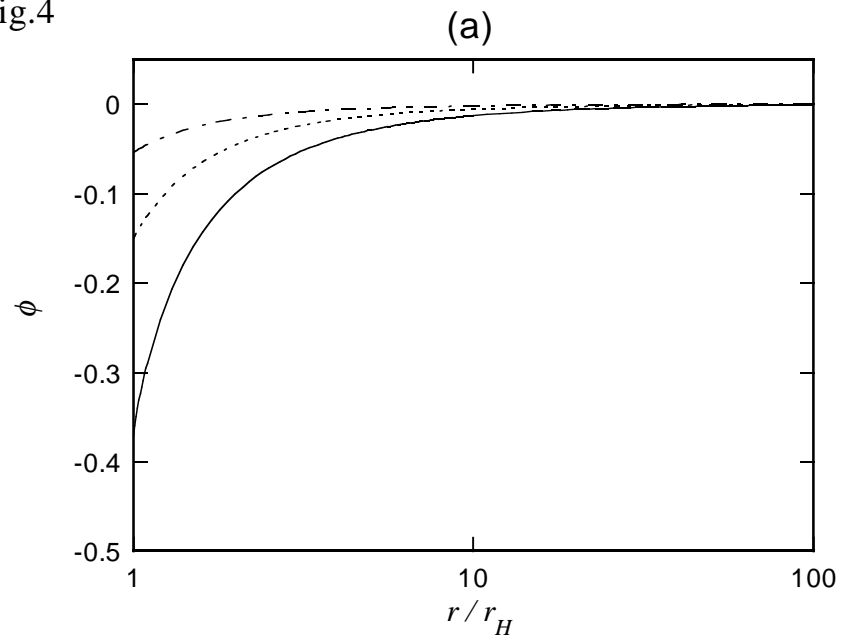


Fig.5

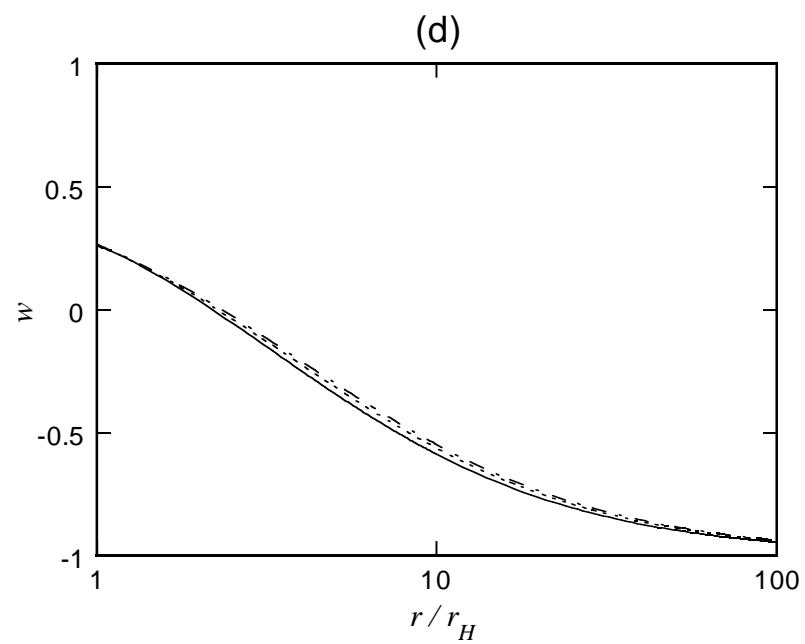
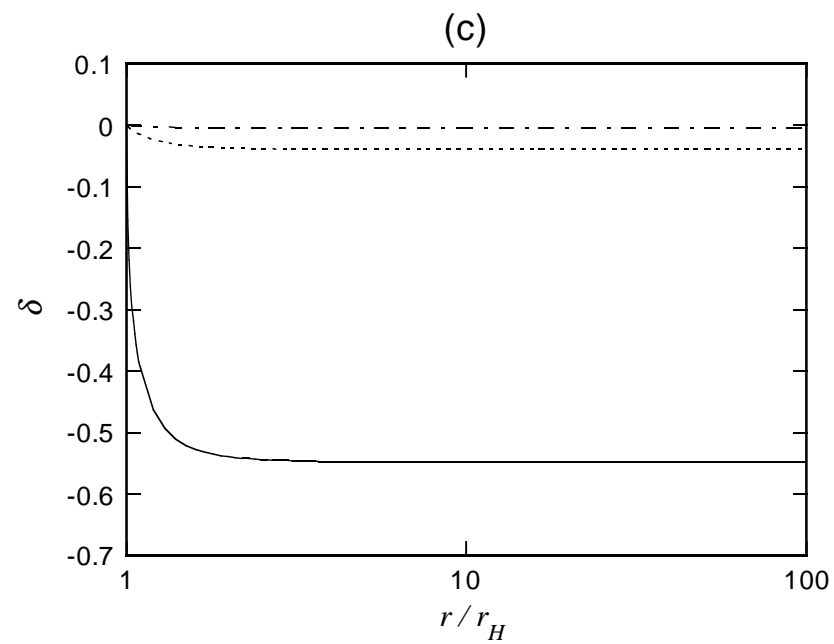
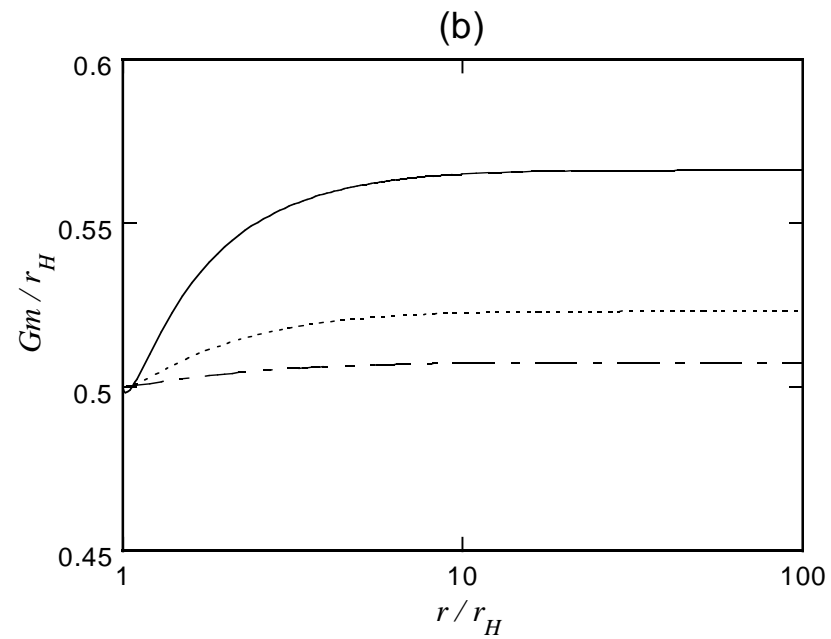
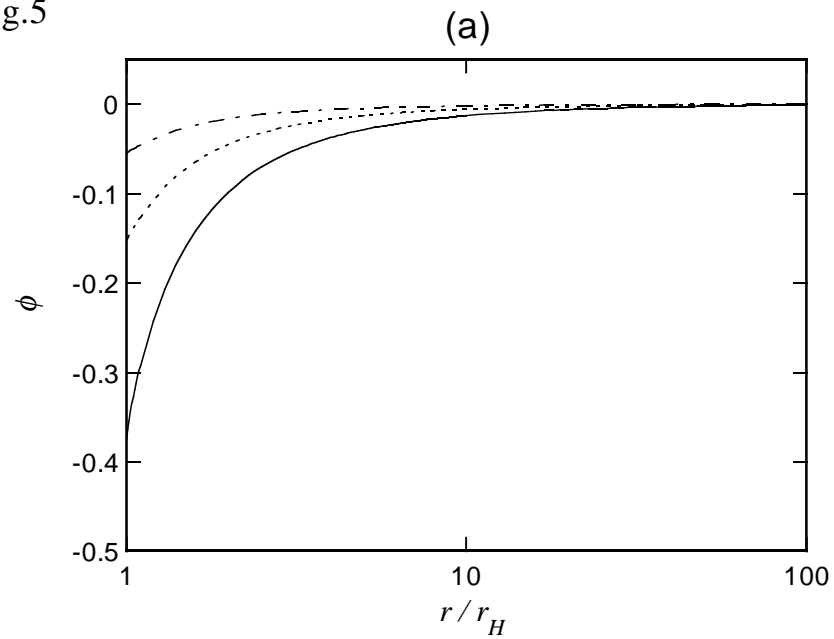


Fig.6

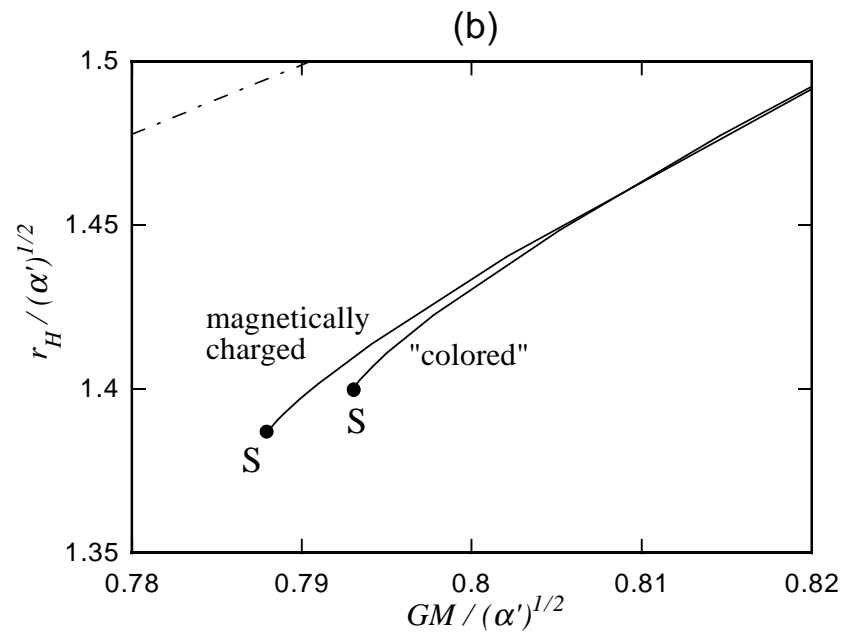
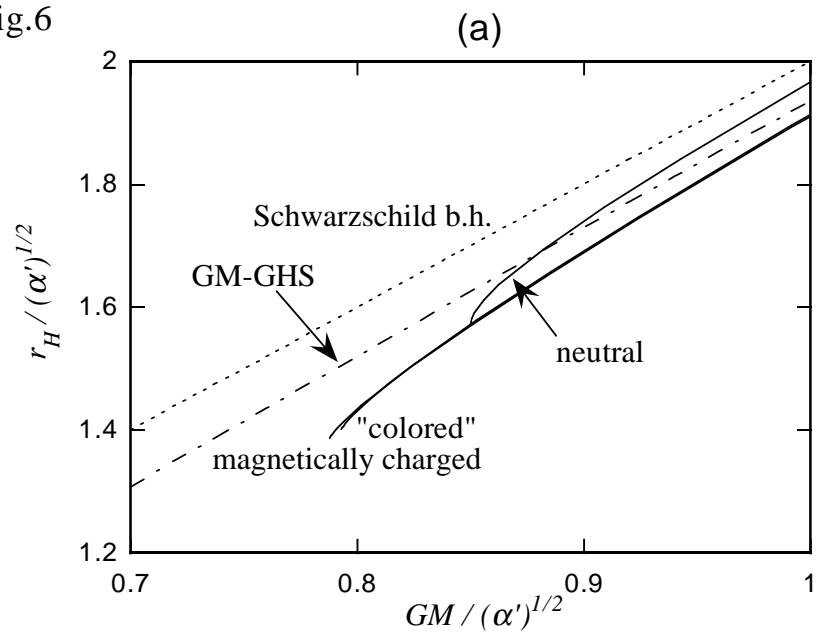


Fig.7

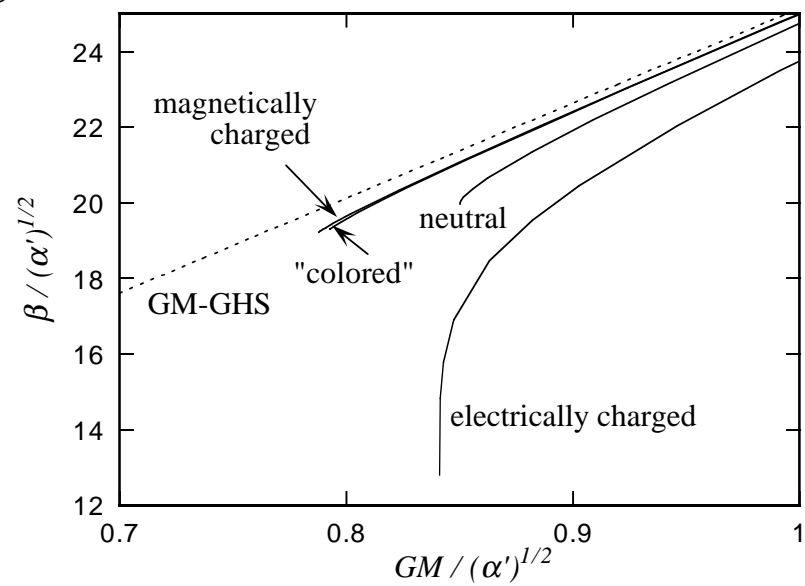


Fig.8

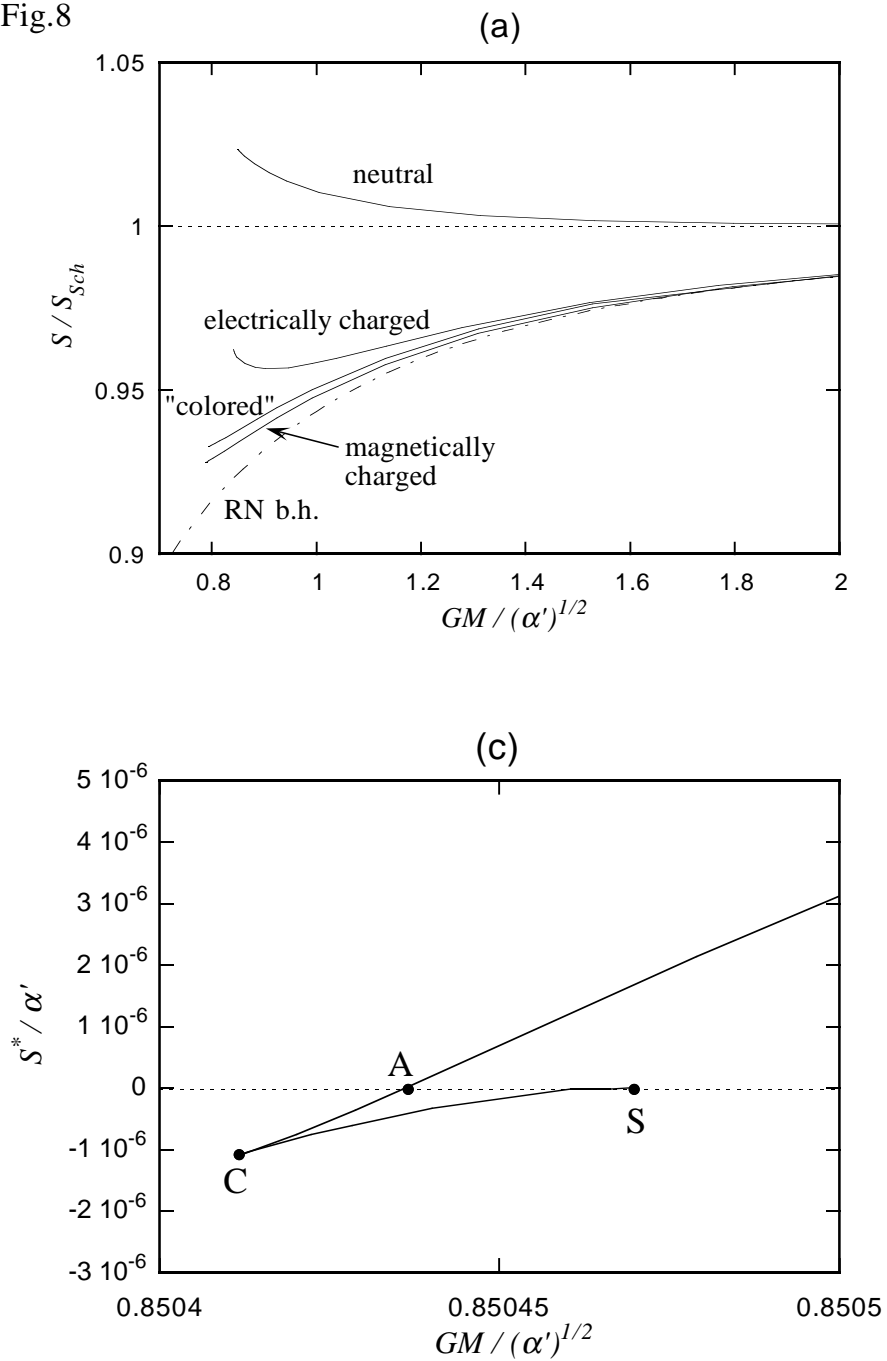


Fig.9

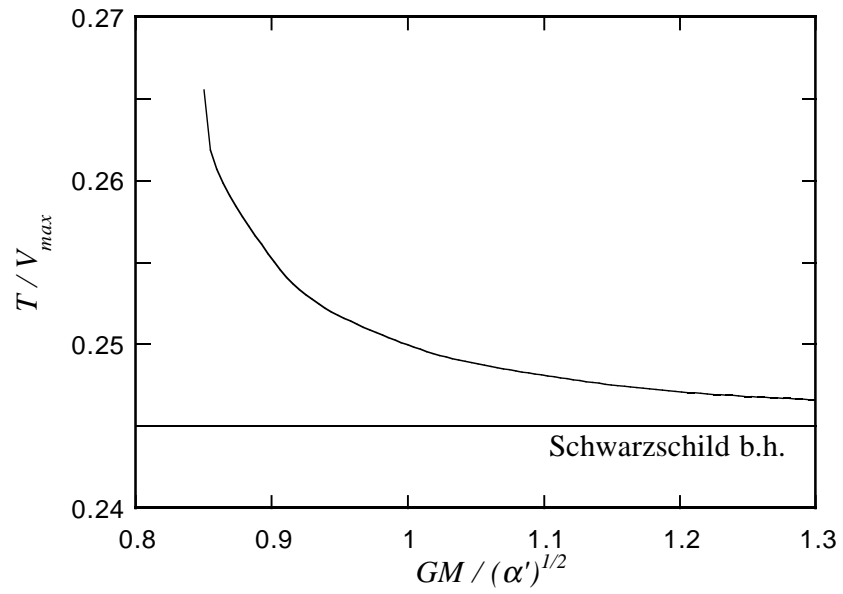


Fig.10

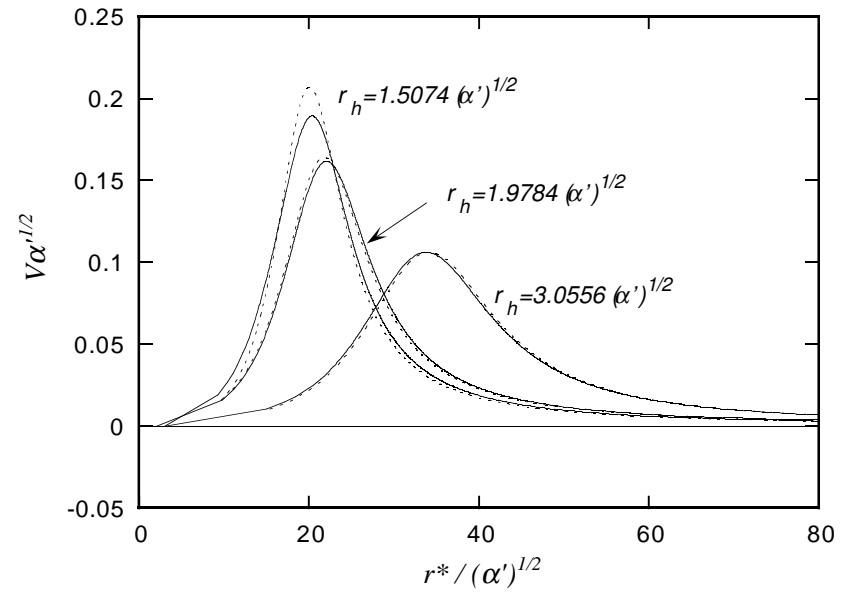


Fig.11

